J. Parasitol., 89(6), 2003, pp. 1191–1205

MOLECULAR PHYLOGENY AND SURFACE MORPHOLOGY OF MARINE ASEPTATE GREGARINES (APICOMPLEXA): *SELENIDIUM* SPP. AND *LECUDINA* SPP.

B. S. Leander, J. T. Harper, and P. J. Keeling

Canadian Institute for Advanced Research, Program in Evolutionary Biology, Department of Botany, #3529-6270 University Boulevard, University of British Columbia, Vancouver, British Columbia, Canada V6T 1Z4. *e-mail: bleander@interchange.ubc.ca*

ABSTRACT: Many aseptate gregarines from marine invertebrate hosts are thought to have retained several plesiomorphic characteristics and are instrumental in understanding the early evolution of intracellular parasitism in apicomplexans and the phylogenetic position of cryptosporidians. We sequenced the small-subunit (SSU) ribosomal RNA genes from 2 archigregarines, *Selenidium terebellae* and *Selenidium vivax*, and 2 morphotypes of the marine eugregarine *Lecudina polymorpha*. We also used scanning electron microscopy to investigate the surface morphology of trophozoites from *Lecudina tuzetae*, *Monocystis agilis*, the 2 species of *Selenidium*, and the 2 morphotypes of *L. polymorpha*. The SSU ribosomal DNA sequences from *S. vivax* and *L. polymorpha* had long branch lengths characteristic of other gregarine sequences. However, the sequence from *S. terebellae* was not exceptionally divergent and consistently emerged as 1 of the earliest 'true' gregarines in phylogenetic analyses. Statistical support for the sister relationship between *Cryptosporidium* spp. and gregarines was significantly bolstered in analyses including the sequence from *S. terebellae* but excluding the longest branches in the alignment. Eugregarines formed a monophyletic group with the neogregarine *Ophryocystis*, suggesting that trophozoites with elaborate cortex folds and gliding motility evolved only once. The trophozoites from the 2 species of *Selenidium* shared novel transverse striations but differed from one another in overall cell morphologies and writhing behavior.

The apicomplexa is a group of obligate unicellular parasites that includes some of the most infamous and well-studied pathogens of vertebrates, e.g., *Plasmodium* spp., *Toxoplasma* spp., and *Babesia* spp. Most apicomplexans, however, are relatively innocuous and, partly for this reason, are poorly understood, making inferences about the evolutionary history of the group difficult. Small-subunit ribosomal DNA (SSU rDNA) phylogenies suggest that apicomplexans are evolutionarily derived from colpodellidlike ancestors, i.e., unicellular biflagellates having an apical complex used in a mode of feeding called myzocytosis (Schnepf and Deichgraber, 1984; Myl'nikov, 1991, 2000; Brugerolle, 2002; Kuvardina et al., 2002; Leander and Keeling, 2003). Whereas both colpodellids and apicomplexans use an apical complex to penetrate and access the cytoplasm of other eukaryotic cells, the transitional steps between free-living predator and obligate intracellular parasite are far from clear. A diverse subgroup of apicomplexans, the Gregarinia, is thought to possess lineages with a number of plesiomorphic characteristics (character states in extant species that have been retained from inferred ancestors) (Théodoridès, 1984; Vivier and Desportes, 1990; Cox, 1994), so phylogenetic studies on gregarines could have a significant impact on inferences about the evolution of intracellular parasitism and improve our understanding of the fundamental properties of apicomplexans as a whole.

Gregarines have monoxenous life cycles in invertebrate hosts and extracellular trophozoite stages that are remarkably diverse in both morphology and behavior (Perkins et al., 2002). Perhaps the most obvious feature of many trophozoites under the light microscope is the presence of ectoplasmic septa between cell regions. Septate gregarines often have a distinctive attachment structure called an epimerite and tend to be found in terrestrial hosts such as insects. Aseptate gregarines possess a single-cell compartment and a less distinctive attachment structure called a mucron and tend to be found in marine hosts such as annelids, molluscs, sipunculids, and urochordates. Trophozoites are the most frequently encountered stage in the gregarine life cycle, so comparative studies on trophozoite morphology not only provide insights into gregarine evolution but also facilitate a utilitarian classification scheme for the group.

Gregarines are traditionally classified into 3 main groups largely based on convenience, i.e., archigregarines, eugregarines, and neogregarines (Grassé, 1953). Archigregarines and neogregarines were once lumped together as schizogregarines because they were all thought to possess merogony, i.e., asexual cell multiplication in either sporozoites or trophozoites (Levine, 1971). Archigregarines (type genus *Selenidium* [Grassé, 1953]) are aseptate, inhabit marine invertebrates and, as the name implies, are thought to possess many plesiomorphic features, such as indistinguishable sporozoite and trophozoite stages. Although there is debate in the literature as to what constitutes archigregarines (Levine, 1971), we prefer the scheme advocated by Schrével (1971a, 1971b), which emphasizes the morphological features of trophozoites rather than the presence or absence of merogony. Neogregarines (type genus *Ophryocystis* [Grassé, 1953]) are often thought to be the most derived gregarines because they inhabit a wide array of insects and usually possess septate trophozoites. Any gregarine, regardless of being aseptate or septate, that appeared to lack merogony was generally lumped into the eugregarines. However, providing evidence for the presence or absence of merogony is difficult to achieve (Ray, 1930; Levine, 1974; Vivier, 1975; Desportes and Théodoridès, 1979; Gunderson and Small, 1986). To accelerate the characterization of gregarine biodiversity, it is more desirable to define taxa based on the presence of easily observable characteristics. In this context, the cortex morphology of trophozoites, as viewed by electron microscopy, will provide an important source of comparative data to meet these basic taxonomic objectives.

Well over 400 species of aseptate gregarines (Levine, 1976) have been described using light microscopy (LM), yet they are the least understood of all gregarines because of their presence in marine worms and their distant connection to human welfare. Nonetheless, aseptate gregarines may be the most important lineages for understanding early apicomplexan evolution and the phylogeny of *Cryptosporidium* spp., intestinal parasites of vertebrates (including humans) (Fayer et al., 1997). Previous molecular phylogenies suggest that *Cryptosporidium* spp. are ear-

Received 19 December 2002; revised 6 May 2003; accepted 6 May 2003.

ly-diverging apicomplexans that are more closely related to gregarines than to coccidians sensu stricto (Carreno et al., 1999; Leander et al., 2003). The addition of sequences from a variety of aseptate gregarines should help clarify the phylogenetic position of *Cryptosporidium* spp. within the Apicomplexa as well as provide a broader framework for tracing character evolution within the group.

To this end, we have used scanning electron microscopy (SEM) to characterize the surface morphology of a number of aseptate gregarines: *Selenidium terebellae* (Kölliker) Ray, *Selenidium vivax* Gunderson and Small, 2 morphotypes of *Lecudina polymorpha* Shrével, *L. tuzetae* Shrével, and *Monocystis agilis* Stein. To place the morphological data into a phylogenetic context and to further evaluate the phylogenetic position of *Cryptosporidium parvum*, we have also sequenced the SSU ribosomal RNA (rRNA) gene from the 2 species of *Selenidium* and the 2 morphotypes of *L. polymorpha* (GenBank AY196706-9). This comparative approach enabled us to address whether species of *Selenidium* (archigregarines) are among the earliest diverging apicomplexans and whether *Selenidium* and *Lecudina* represent monophyletic groups. Moreover, we provide a preliminary framework for tracing character evolution in the group and for evaluating whether trophozoite cortex morphology reflects phylogenetic relationships, as inferred from SSU rDNA.

MATERIALS AND METHODS

Collection and identification of organisms

Marine invertebrate hosts were collected at low tide (0.2–0.3 m above the mean low tide) from the intertidal mudflats and rocky pools of Grappler Inlet near Bamfield Marine Station, Vancouver Island, Canada, in April 2002. Trophozoites from a species of *Selenidium* were isolated from the intestines of a terebellid polychaete, *Thelepus* sp. These gregarines fit the description of *S. terebellae* (Ray, 1930) and accordingly are designated as such hereafter. Trophozoites that conformed exactly to the species description of *S. vivax* were isolated from the intestines of the sipunculid *Phascolosoma agassizii* Keferstein (Gunderson and Small, 1986).

Two different *Lecudina*-like morphotypes coinhabited the intestines of a species of the polycheate *Lumbrineris* (syn. *Lumbriconereis*). The trophozoites of 1 of these morphotypes, designated as morphotype 2, frequently possessed an elongated mucron and were very similar to the descriptions of *L. heterocephala* Mingazzini and *L. polymorpha* Schrével (Schrével, 1963, 1969). Even though the second morphotype, designated as morphotype 1, was shorter and lacked an elongated mucron, it seemed more similar to morphotype 2 than to any species description of *Lecudina* we encountered (Levine, 1976). Altogether, the gregarines we observed in *Lumbrineris* sp. conformed best to the description of *L. polymorpha* because this gregarine was also isolated from *Lumbrineris* hosts (*L. heterocephala* was described from the polycheate *Nephtys* sp.) and consisted of a range of morphological forms that could reasonably account for both morphotypes (Schrével, 1963, 1969). Accordingly, we have designated the 2 morphotypes as *Lecudina polymorpha* morphotype 1 and *Lecudina polymorpha* morphotype 2.

Two other aseptate gregarines were further examined in this study, i.e., *Lecudina* sp. (Leander et al., 2003) and *M. agilis*. It is now apparent by closely examining the species descriptions by Schrével (1963, 1969) that the gregarine and SSU rDNA sequence reported in Leander et al. (2003) as *Lecudina* sp. (AF457128) can be more confidently linked to *L. tuzetae*. This gregarine was isolated from the gut of the marine polychaete *Nereis vexillosa* collected at low tide in Stanley Park, Vancouver, British Columbia, Canada, in September 2001. Trophozoites of *M. agilis* were isolated from the seminiferous vesicles of earthworms (*Lumbricus terrestris*) purchased from Berry's Bait and Tackle (Richmond, British Columbia, Canada).

Microscopy

Light microscopy: A Meiji dissecting microscope (Meiji Techno Co., Ltd., Tokyo, Japan) and a Zeiss Axiovert 200 inverted microscope facilitated the micromanipulation of individual trophozoites. Light micrographs were produced by securing trophozoites under a coverslip with VALAP (1 vaseline:1 lanolin:1 paraffin [Kuznetsov et al., 1992]) and viewing them with a Zeiss Axioplan 2 Imaging microscope connected to a Q-Imaging, Microimager II, black and white digital camera.

Scanning electron microscopy: Trophozoites from each gregarine species were released into seawater by teasing apart the intestine of their respective hosts with fine-tipped forceps. For each species, 10–20 parasites were removed from the remaining gut material by micromanipulation and washed twice in filtered seawater. Individual trophozoites were deposited directly into the threaded hole of a Swinnex filter holder, containing a 5-μm polycarbonate membrane filter (Coring Separations Division, Acton, Massachusetts) submerged in 10 ml of seawater within a small canister (2 cm in diameter and 3.5 cm tall). Whatman filter paper, mounted on the inside base of a beaker (4 cm in diameter and 5 cm tall), was saturated with 4% OsO_4. The beaker was placed over the canister, and the parasites were fixed by OsO_4 vapors for 30 min. Six drops of both 8% gluataraldehyde and 4% OsO_4 were added directly to the seawater and the parasites were fixed for an additional 30 min. A 10-ml syringe filled with distilled water was screwed to the Swinnex filter holder, and the entire apparatus was removed from the canister containing seawater and fixative. The trophozoites were dehydrated with a graded series of ethyl alcohol and critical point dried with CO_2. Filters were mounted on stubs, sputter coated with gold, and viewed under a Hitachi S4700 scanning electron microscope (*L. tuzetae* was viewed with a much older Cambridge 250T scanning electron microscope). Some SEM micrographs were created from montages of 3–8 individual images of the same cell and presented on black backgrounds using Adobe Photoshop 6.0 (Adobe Systems, San Jose, California).

DNA isolation, amplification, cloning, and sequencing

Approximately 40 trophozoites of each species (and morphotype of *L. polymorpha*) were isolated, washed 3 times in filtered seawater, and deposited into an Eppendorf tube. DNA was extracted by suspending pelleted material in 100 μl CTAB extraction buffer (1.12 g Tris, 8.18 g NaCl, 0.74 g ethylenediaminetetraacetic acid, 2 g CTAB, 2 g polyvinylpyrolidone, 0.2 ml 2-mercaptoethanol in 100 ml water; Zolan and Pukkila, 1986) in a Knotes Duall 20 tissue homogenizer. The material was incubated at 65 C for 30 min with periodic grinding and separated with chloroform–isoamyl alcohol (24:1); the aqueous phase was then precipitated in 95% ethanol.

SSU rRNA genes were amplified using polymerase chain reaction (PCR) primers and a thermocycling protocol described previously for individually isolated gregarines (Leander et al., 2003). PCR products corresponding to the expected size were gel isolated and cloned into the pCR 2.1 vector using the TOPO TA cloning kit (Invitrogen, Frederick, Maryland). At least 32 clones from each product were screened for size using PCR and digested with *Sau*3AI to group the products by the restriction pattern. Two to 4 clones from each restriction pattern were sequenced with ABI big-dye reaction mix using the vector primers and 4 internal primers oriented in both directions. Sequences derived from metazoan hosts were detected by BLAST analysis. New gregarine sequences were deposited in GenBank.

Molecular phylogenetic analysis

Alignments: Four different alignments were constructed using MacClade 4 (D. R. Maddison and W. P. Maddison, 2000). Sequences from *S. vivax*, *S. terebellae*, *Lecudina polymorpha* morphotype 1, and *Lecudina polymorpha* morphotype 2 (GenBank accession numbers listed below) were added to an existing alignment consisting of diverse alveolates, including previously published gregarines, colpodellids, and representatives from other major eukaryotic groups—a 72-taxon alignment containing 1,312 sites. However, more comprehensive analyses were achieved by focussing on 3 smaller alignments. A 40-taxon alignment containing 1,408 sites consisted of 37 in-group taxa (representative alveolates) and 3 out-group taxa (representative stramenopiles). To further examine the relationship between *Cryptosporidium* spp. and gregarines, a 34-taxon alignment containing 1,435 sites was produced by removing the 6 most divergent branches in the 40-taxon alignment:

Gregarina niphandrodes Clopton et al., *Leidyana migrator* Clopton, *L. tuzetae*, *Lecudina polymorpha* morphotype 1, *Lecudina polymorpha* morphotype 2, and *S. vivax*. The relationship between gregarines and *Cryptosporidium* spp. was also examined by adding 4 more sequences from different species of *Cryptosporidium* (*Cryptosporidium baileyi*, *Cryptosporidium muris*, *C. parvum*, and *Cryptosporidium wrairi*) to the 34-taxon alignment, producing a 38-taxon alignment consisting of 1,430 sites.

Phylogenetics: Maximum likelihood (ML) and distance methods under different DNA substitution models were performed on the alignments. The alpha-shape parameters for site-to-site rate variation were estimated from the data using the HKY model and a gamma distribution with an invariable sites parameter and 8 rate categories (0.31 for the 72-taxon alignment, 0.62 for the 40-taxon alignment, 0.51 for the 34-taxon alignment, and 0.52 for the 38-taxon alignment; fraction of invariable sites was 0.00 for all alignments). Corrected ML trees were constructed with PAUP* 4.0 using the general time-reversible (GTR) model for base substitutions (Posada and Crandall, 1998; Swofford, 1999). For the 40-taxon and 34-taxon alignments, ML bootstrap analyses were performed in PAUP* (Swofford, 1999) on 100 resampled data sets under an HKY model using corrections for site-to-site rate variation estimated from the original data set.

Distances for all 4 SSU rDNA data sets were calculated with TREE-PUZZLE 5.0 using the HKY substitution matrix (Strimmer and Von Haeseler, 1996) and with PAUP* 4.0 using the GTR model. Distance trees were constructed with minimum evolution (using GTR) in PAUP* (Swofford, 1999) and weighted neighbor joining using Weighbor (Bruno et al., 2000). One hundred bootstrap data sets were generated with SEQBOOT (Felsenstein, 1993), and respective distances were calculated with the shell script 'puzzleboot' (M. Holder and A. Roger, www.tree-puzzle.de) using the alpha-shape parameter and transition–transversion ratios estimated from the original data sets.

We also analyzed the 40- and 34-taxon data sets with parsimony. Nucleotides were treated as independent, unordered, character states of equal weight, and gaps were treated as missing data. A heuristic search was performed using PAUP* 4.0 with ACCTRAN character state optimization, tree bisection–reconnection branch swapping, random stepwise addition of taxa, and MULTREES on. Nonparametric bootstrap values from 500 replicates were generated to evaluate the robustness of each node on the most parsimonious tree(s). The tree length, number of most parsimonious trees, number of informative characters, consistency indices (CI), and retention indices (RI) were reported.

GenBank accession numbers: AF069516, *Amoebophrya* sp.; AF274256, *Amphidinium semilunatum*; AF158702, *Babesia gibsoni*; M97909, *Blepharisma americanum*; AF060975, *Caryospora bigenetica*; AY142075, *Colpodella* sp.; American Type Culture Collection 50594, AY078092, *Colpodella pontica*; X53229, *Costaria costata*; AF080097, *Cryptoperidiniopsis brodyi*; L19068, *C. baileyi*; L19069, *Cryptosporidium andersoni*; AF093489, *C. parvum*; AF093502, *Cryptosporidium serpentis*; U11440, *C. wrairi*; U57771, *Didinium nasutum*; AF239261, *Dinophysis norvegica*; AF231803, *Durinskia baltica* (formerly *Peridinium balticum*); AF291427, *Eimeria alabamensis*; AJ402349, eukaryote clone OLI11005; X65150, *Furgasonia blochmanni*; AF129882, *G. niphandrodes*; AF274261, *Gyrodinium dorsum*; AF286023, *Hematodinium* sp.; AF297085, *Hepatozoon* sp.; AF274268, *Kryptoperidinium foliaceum*; AY196706, *Lecudina polymorpha* morphotype 1; AY196707, *Lecudina polymorpha* morphotype 2; AF457128 as *Lecudina* sp., *L. tuzetae*; AF457130, *L. migrator*; M87333, *Mallomonas striata*; U07937, marine clone from *Ammonia beccarii*; AB000912, marine parasite from *Tridacna crocea*; AF457127, *M. agilis*; AF022200, *Noctiluca scintillans*; AF129883, *Ophryocystis elektroscirrha*; M14601, *Oxytricha nova*; AF126013, *Perkinsus marinus*; Y16239, *Prorocentrum emarginatum*; AF194409, *Protocruzia* sp.; AF274275, *Pyrodinium bahamense*; AY196709, *S. terebellae*; AY196708, *S. vivax*; AF236097, *Theileria buffeli*; AB022111, *Thraustochytrium multirudimentale*; M97703, *Toxoplasma gondii*; AF255357, *Urocentrum turbo*.

RESULTS

Comparative surface morphology of gregarine trophozoites

Selenidium terebellae: Thirty trophozoites were examined by LM, and 2 were recovered for SEM. Trophozoites were vermiform, 115–160 μm in length, and capable of nematodelike bending movements when detached from the host (Figs. 1, 2). The anterior end appeared to possess an apical complex because it was conoidal in shape and bore ringlike indentations, about 0.2–0.3 μm in diameter, positioned terminally where rhoptries would be expected to dock within the conoid (Figs. 9, 10). The trophozoite surface was scored with 4–6 longitudinal grooves that twisted slightly near the ends of the cell (Fig. 9). The longitudinal grooves terminated before reaching the apex of the dome-shaped posterior end (Fig. 12). The surfaces between the grooves, interpreted as large 'folds' (8–10 μm in width), possessed transverse striations that took the form of weakly raised ripples with a periodicity of 1 per 3 μm (Figs. 9, 11). The surface of the trophozoites was also covered with fine particles, with a diameter ranging from 0.05 to 0.3 μm (Figs. 10–12).

Selenidium vivax: Thirty trophozoites were examined by LM, and 3 were recovered for SEM. Trophozoites were capable of extreme contortion when detached from the host (Figs. 3–5, 13). The relaxed stages were extremely flat, 150–425 μm in length, and 50–75 μm wide (Fig. 3). When observing the trophozoites from the side (thin view), the large, single nucleus bulged outward. Contracted stages were about 60–80 μm in length and 50–75 μm wide (Figs. 4, 16). The anterior end was usually asymmetrical with a straight edge about 15–25 μm across (Figs. 13, 16), but more contorted morphologies were also observed. The shape of the posterior end ranged from rounded to somewhat pointed, as viewed from the widest side of trophozoites. Delicate longitudinal striations were visible near both ends of the trophozoites and in regions that appeared stretched along the longitudinal axis of the cell. Roughly 12–15 longitudinal striations were visible on the widest sides of the trophozoites (Figs. 3, 13). Raised transverse striations that varied considerably in length (5 μm to well over 30 μm long and 0.5 μm in diameter) were visible only using SEM (Figs. 13–16). In many cases, the terminal ends of the striations appeared fused to the surface membrane (Fig. 14), but in other cases the striations appeared to dangle from the cell surface (Fig. 15). These transverse striations occurred over the posterior two-thirds of contracted trophozoites (Fig. 16) and in specific regions near the anterior and posterior ends of relaxed trophozoites (Fig. 13).

Lecudina polymorpha: The trophozoites found in the gut of *Lumbrineris* sp. conformed to the species description of *L. polymorpha* and had 2 overlapping morphotypes. Thirty trophozoites from each morphotype were examined by LM, and 10 from each were recovered for SEM. Trophozoites from both morphotypes were rigid, capable of gliding motility, and slightly arched along the longitudinal axis (Figs. 6, 7). The posterior ends of both morphotypes came to a distinct point. Trophozoites from morphotype 1 were usually 175–300 μm in length and 35–50 μm wide (Figs. 6, 17). Trophozoites from morphotype 2 were usually 475–575 μm in length (excluding an elongated mucron) and 35–50 μm wide (Figs. 7, 22). The elongated mucron on some trophozoites from morphotype 2 was usually 75–100 μm in length and 15 μm wide (Figs. 8, 22, 24). The cortex of both morphotypes was covered with extremely fine longitudinal folds that lacked prominent signs of undulation activity; morphotypes 1 and 2 had packing densities of 3 and 5 folds/μm, respectively (Figs. 18, 23). In both morphotypes, many folds terminated before reaching the anterior and posterior ends;

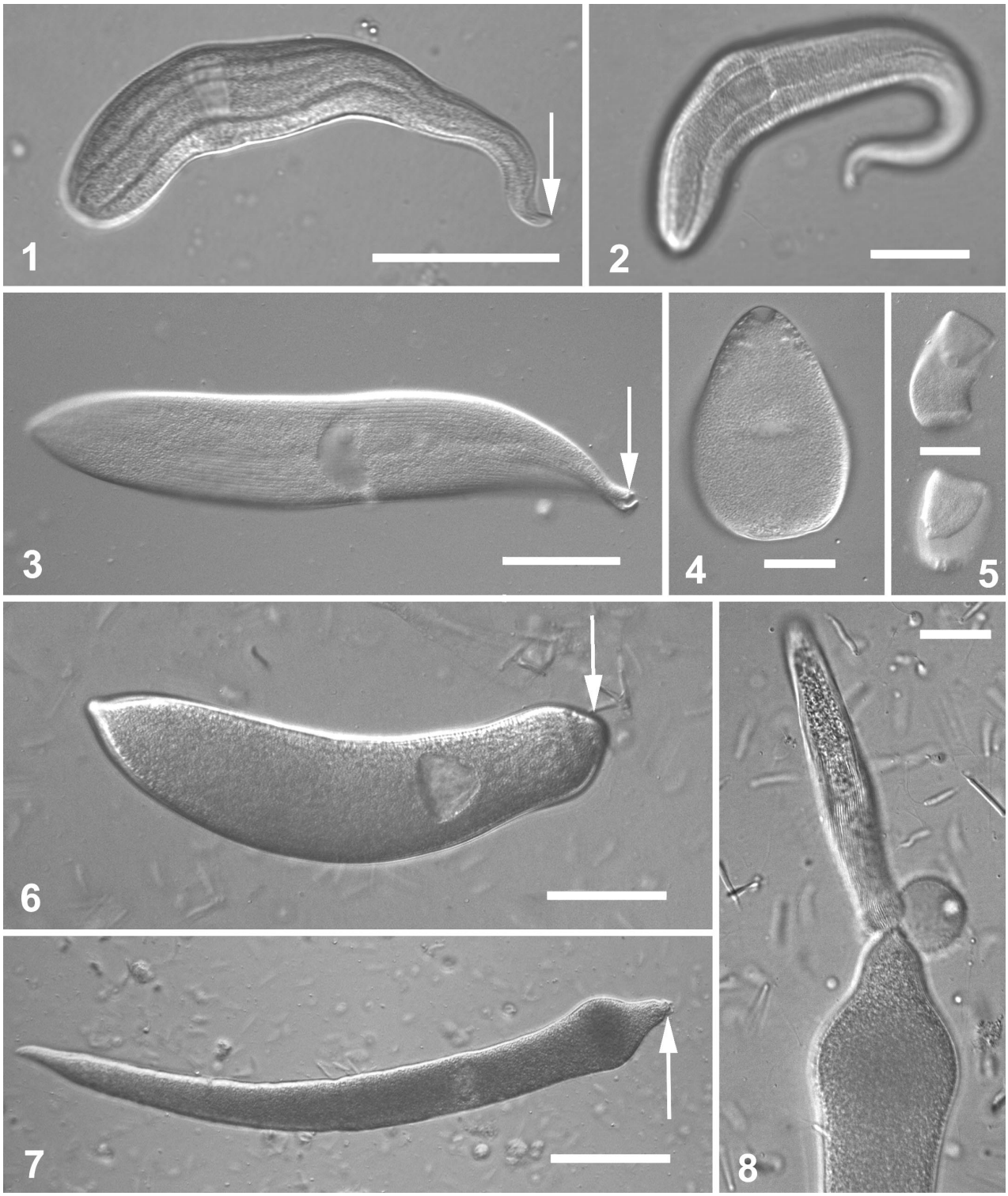

FIGURES 1–8. Light micrographs of trophozoites from the marine gregarines isolated for DNA sequencing and SEM; arrows mark the mucron or anterior ends of each cell. **1–2.** *Selenidium terbellae*. **3.** Relaxed state for trophozoites of *Selenidium vivax*. **4.** Contracted state for trophozoites of *S. vivax*. **5.** Intermediate (bending) states for trophozoites of *S. vivax*. **6.** *Lecudina polymorpha* morphotype 1. **7.** *Lecudina polymorpha* morphotype 2. **8.** The anterior end of *Lecudina polymorpha* morphotype 2 with an elongated mucron. **1, 3, 5–6:** Bar = 50 μm. **2, 4, 8:** Bar = 25 μm. **7:** Bar = 100 μm.

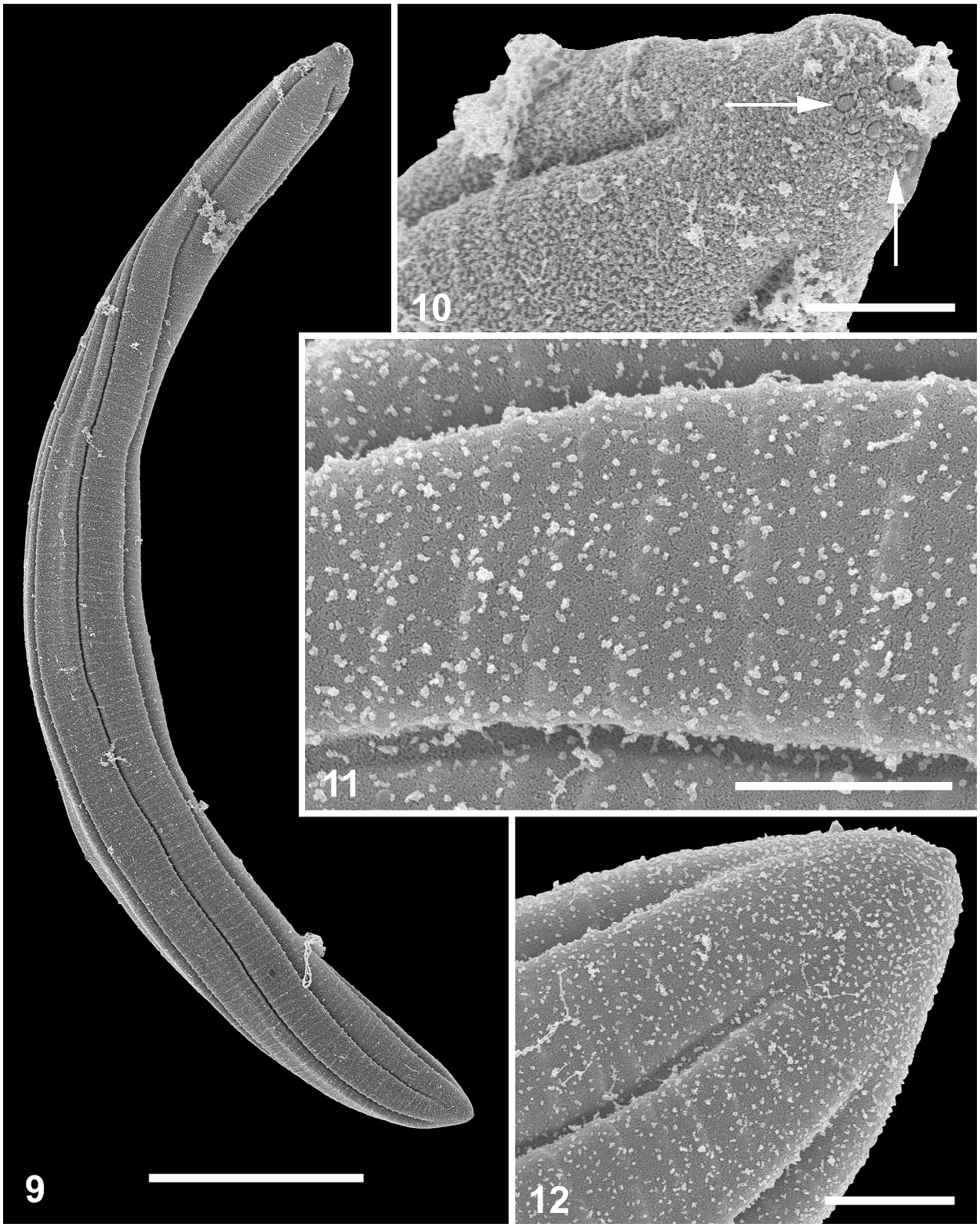

FIGURES 9–12. Scanning electron micrographs of *Selenidium terebellae*. **9.** A crescent-shaped trophozoite showing a rigid conoidlike mucron (top end), transverse striations across the cortex folds, and 4 grooves running longitudinally along the cell. **10.** High-magnification view of the mucron showing what appears to be docking sites for rhoptries (arrows). **11.** High-magnification view of the cortex folds showing transverse striations in the form of subtle elevated ridges (running vertically). **12.** High-magnification view of the posterior end of the trophozoite showing the termination of 3 grooves. **9:** Bar = 20 μm. **10, 12:** Bar = 2.5 μm. **11:** Bar = 5 μm.

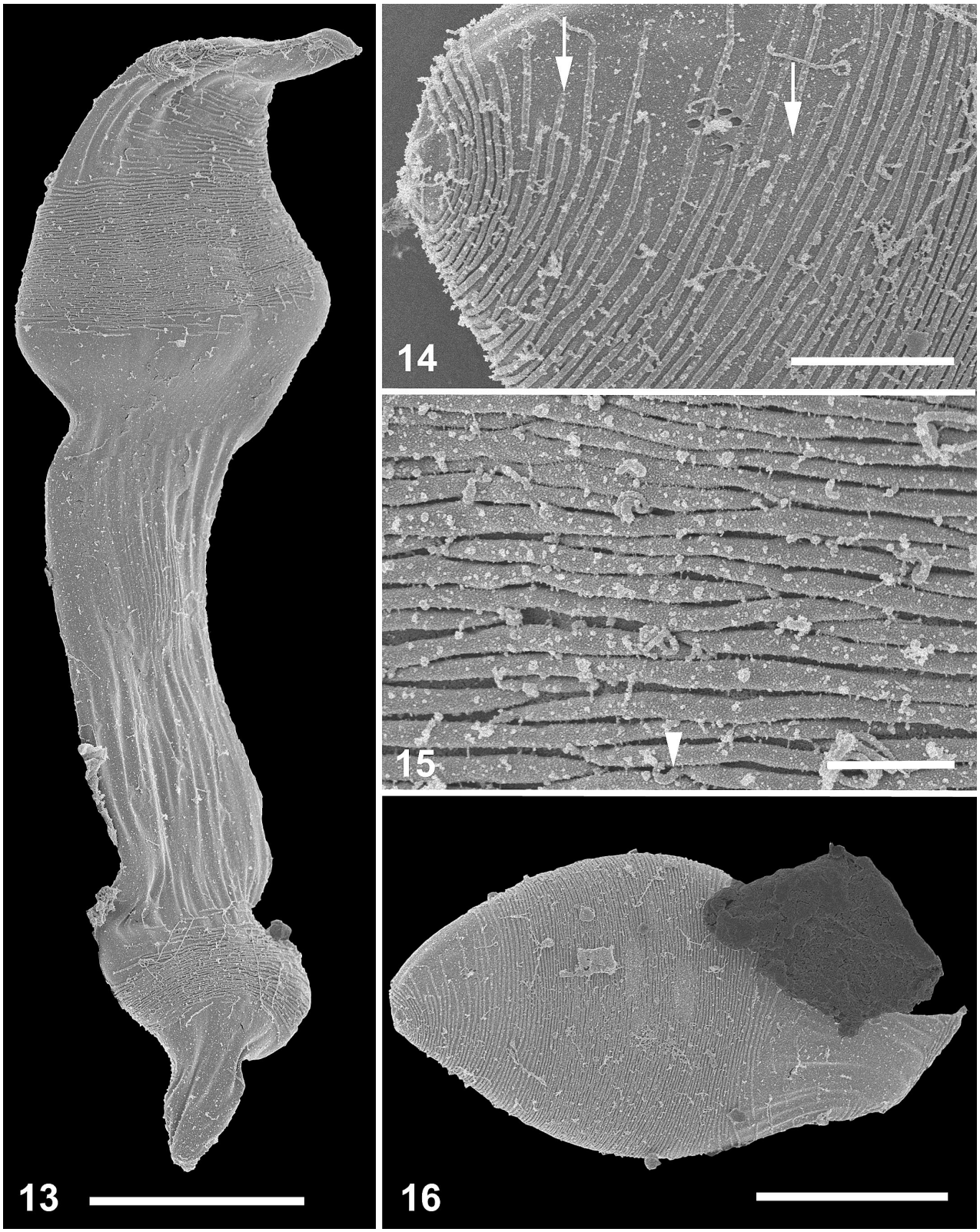

FIGURES 13–16. Scanning electron micrographs of *Selenidium vivax*. **13.** A trophozoite showing a flattened and deformed cell shape indicative of twisting behavior observed under the light microscope. The image also shows an asymmetrical mucron or 'rostrum' (positioned at the top end of the cell), transverse striations near each end of the cell, and fine longitudinal striations across the surface of the midcell region. **14.** High-magnification view of a trophozoite showing that the ends of the raised transverse striations usually appear fused to the plasma membrane (arrows). **15.** Higher-magnification view showing that occasionally the ends of the transverse striations (arrowhead) dangle from the cell surface. **16.** The contracted state for trophozoites showing the asymmetrical mucron oriented to the right (a large particle of debris has been artificially darkened for clarity); notice that the transverse striations cover the posterior two-thirds of the cell surface. **13:** Bar = 25 μm. **14:** Bar = 5 μm. **15:** Bar = 1.5 μm. **16:** Bar = 20 μm.

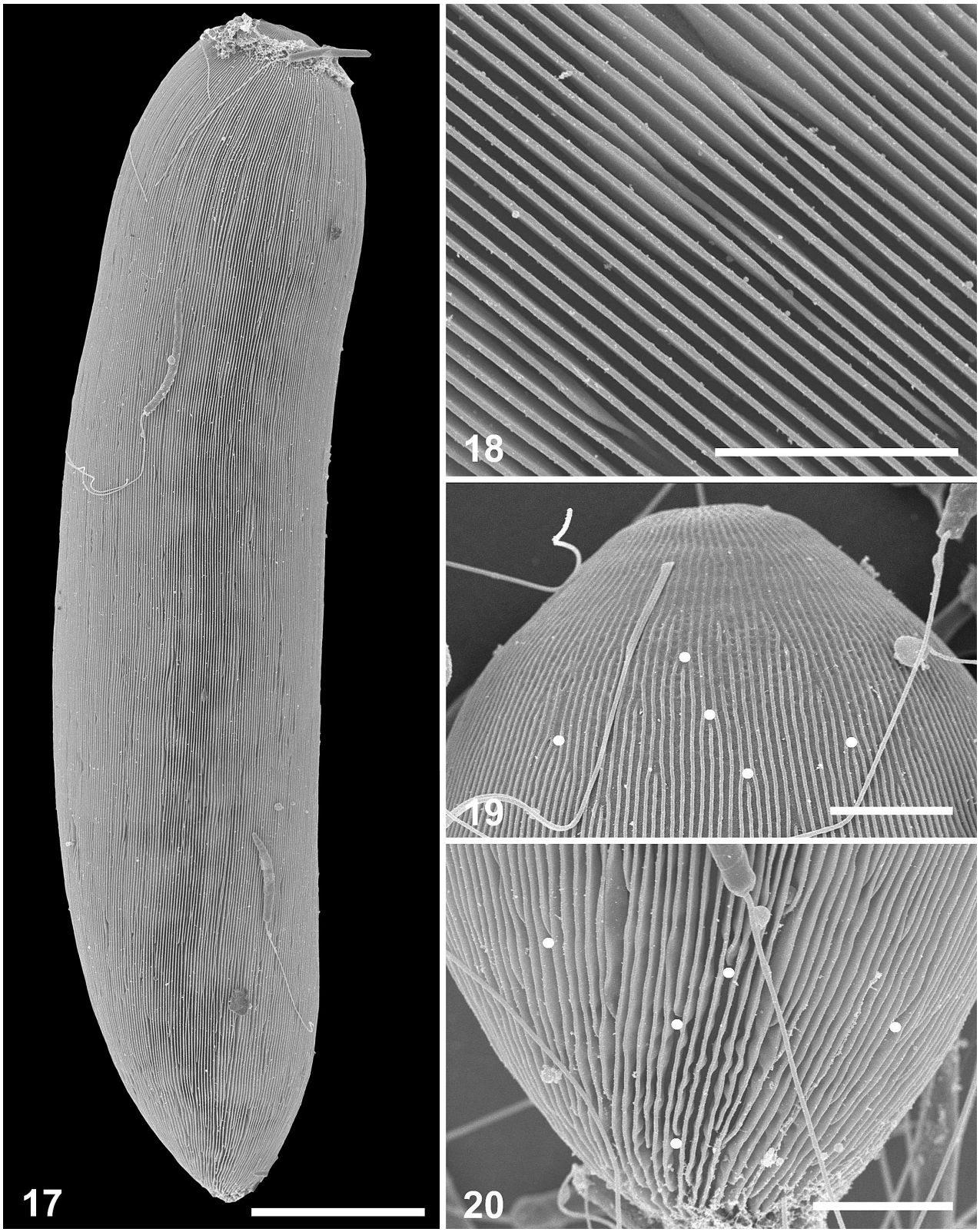

FIGURES 17–20. Scanning electron micrographs of *Lecudina polymorpha* morphotype 1. **17.** A trophozoite showing approximately 100 longitudinally arranged cortex folds (anterior end is at the top). **18.** High-magnification view of the cortex folds showing a general lack of undulations and a density of 3 folds/μm. **19.** High-magnification view of the mucron showing folds that terminate before reaching the anterior cell apex (circles). **20.** High-magnification view of the trophozoite showing folds that terminate before reaching the posterior cell apex (circles). **17:** Bar = 25 μm. **18–20:** Bar = 5 μm.

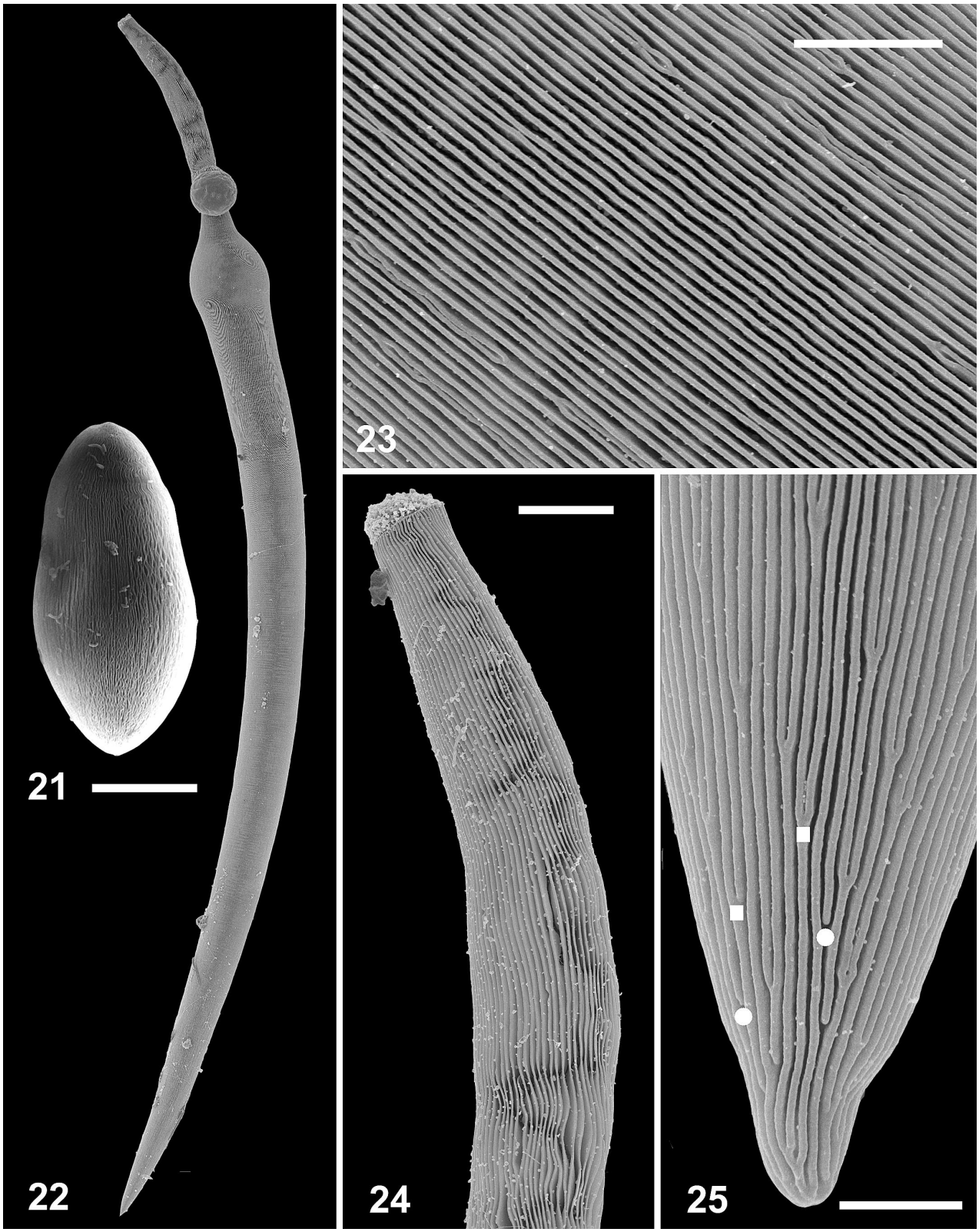

FIGURES 21–25. Scanning electron micrographs of *Lecudina tuzetae* and *Lecudina polymorpha* morphotype 2 showing the morphological extremes in the currently recognized genus. **21.** A trophozoite of *L. tuzetae* (image taken with a much older Cambridge 250T scanning electron microscope). **22.** A trophozoite of *L. polymorpha* morphotype 2 showing an elongated mucron (top end) and a pointed posterior tip (bottom end). **23.** High-magnification view of *L. polymorpha* morphotype 2 showing a general lack of undulations in the cortex folds and a density of 5 folds/ μm. **24.** High-magnification view of the elongated mucron in *L. polymorpha* morphotype 2 showing evidence of undulating folds all of which terminate at the anterior cell apex. **25.** High-magnification view of the trophozoite showing folds that both terminate (circles) and bifurcate (squares) before the posterior cell apex. **21–22:** Bar = 50 μm. **23:** Bar = 2.5 μm. **24:** Bar = 5 μm. **25:** Bar = 1.5 μm.

however, no obvious pattern was noticeable (Figs. 20, 25). The folds of morphotype 2 also produced bifurcations across the cortex that were particularly abundant near the pointed posterior end and the base of the mucron (Figs. 23, 25), but no obvious pattern of fold bifurcations was observed. The folds on the elongated mucron of morphotype 2 showed subtle signs of undulations and had a density of 3 folds/μm (Fig. 24). All the folds of this structure terminated on a common ring at the distal end. Shortly after removing the trophozoites of morphotype 2 from the host, a sphere of unknown material oozed out from the proximal junction of the elongated mucron (Figs. 8, 22).

Lecudina tuzetae: Thirty trophozoites were examined by LM, and 1 was recovered for SEM. The trophozoites of the taxon were rigid, capable of gliding motility, and usually 100–150 μm in length and 60 μm wide (Fig. 21). The cell cortex was covered with numerous folds oriented longitudinally and with a density of 2 folds/μm. The folds took on an alternating pattern, where every undulating fold was bordered on either side by a straight fold, a pattern demonstrated clearly in a very similar marine gregarine, *Lecudina pellucida* (Vivier, 1968). Folds terminated and bifurcated near the posterior and anterior ends of trophozoites but without any obvious pattern.

Monocystis agilis: Thirty trophozoites from this taxon were examined by LM, and 6 were recovered for SEM. Trophozoites of *M. agilis* were spindle shaped, usually 75–90 μm in length, and about 25–30 μm at the widest transect (Fig. 26). Trophozoites were never observed gliding or bending. The folds of the cortex were relatively large, having a density of about 1 fold/μm (Figs. 26–28). Fold terminations and bifurcations occurred near the anterior and posterior ends but without any discernable pattern (Figs. 27, 28). The anterior and posterior tips were free of folds, and the folds terminated across a distinct ring at the base of the mucron (Fig. 27). Underlying striations radiated from the base of a conelike structure on the mucron; these striations were continuous with the folds of the cell cortex (Fig. 27). The mucron of some trophozoites consisted of 2 or 3 bulbous swellings (Fig. 26).

Phylogeny of gregarines as inferred from SSU rDNA

The 72-taxon data set consisting of representatives from diverse eukaryotic groups helped confirm that the 4 sequences reported in this study were derived from the individually isolated gregarines because they clustered within an apicomplexan clade (data not shown). Like the SSU rDNA sequences from the dinoflagellate *Oxyrrhis marina* and the apicomplexan *Plasmodium falciparum*, most gregarine sequences had extraordinarily long branch lengths, a property known to confound phylogenetic analyses. Despite potential artifacts due to long-branch attraction (LBA), gamma-corrected distance, gamma-corrected ML, and parsimony analyses (tree length [gap, fifth base] = 3,748, number of most parsimonious trees = 83, number of informative characters = 648, CI [excluding uninformative characters] = 0.403, and RI = 0.454) of the 40-taxon data set showed dinoflagellates and apicomplexans as sister groups with high bootstrap support (100/93/96; Fig. 29A). Moreover, *P. marinus* diverged as the earliest sister to dinoflagellates and colpodellids diverged as the earliest sister group to apicomplexans in all analyses, which is consistent with previous results (Kuvardina et al., 2002).

In analyses using multiple sequences from different species of *Cryptosporidium*, the members of the genus clustered tightly together and consistently emerged as the earliest sister group to sequences from unambiguously identified gregarines (analyses of the 38-taxon data set), which is consistent with previous results (Carreno et al., 1999). Accordingly, *C. serpentis* served as the representative for *Cryptosporidium* spp. in all other analyses. In gamma-corrected distance and parsimony analyses, sequences from 2 gregarinelike sequences, the marine parasite from *T. crocea* and the marine clone misattributed to *A. beccarii*, formed the sister group to the true gregarine clade, which is consistent with previous analyses (Leander et al., 2003). By contrast, these sequences did not cluster with the gregarine clade in ML analyses but branched after colpodellids as the sister group to all other apicomplexans; however, there was no statistical support for this position in any of the trees (Fig. 29A).

The 2 sequences from *Selenidium* spp. consistently diverged as the earliest lineages of true gregarines. *Selenidium vivax* diverged before *S. terebellae* in ML analyses (Fig. 29A), but it clustered with the 3 sequences from *Lecudina* spp. in parsimony analyses. Unlike most gregarine sequences, the early-diverging sequence from *S. terebellae* was relatively conserved, making it a potentially useful representative gregarine in phylogenetic analyses, with long-branch sequences excluded. When the most divergent gregarines sequences were removed from the 40-taxon alignment, *C. serpentis* clustered with *S. terebellae*, *M. agilis*, and *O. elektroscirrha* in every analysis with moderate to high statistical support (75/88/91/80; Fig. 29B) (parsimony analysis: tree length [gap, fifth base] = 2,426, number of most parsimonious trees = 6, number of informative characters = 453, CI [excluding uninformative characters] = 0.402, and RI = 0.454).

The 3 clones sequenced from *L. polymorpha* morphotype 1 were identical to each other (GenBank AY196706). One of the 3 clones sequenced from *L. polymorpha* morphotype 2 was identical to the sequences from morphotype 1; the other 2 clones sequenced from morphotype 2 (GenBank AY196707) differed from the previous sequences by only 12 bases (99.3% sequence identity). The near identical sequences from the 2 morphotypes of *L. polymorpha* diverged after *Selenidium* spp. in ML analyses, making it the earliest lineage of gregarines with a complex cortex consisting of numerous folds.

Terrestrial gregarines (*O. elektroscirrha*, *M. agilis*, *G. niphandrodes*, and *L. migrator*) formed a clade exclusive of marine gregarines in parsimony trees, but this clade was interrupted by the marine gregarine *L. tuzetae* in both ML and gamma-corrected distance trees. In the latter trees, *L. tuzetae* was a sister lineage to the septate gregarines: *L. migrator* and *G. niphandrodes*. However, these relationships are weakly supported and very likely prone to artifacts because of LBA. The 2 septate gregarines in the analyses, however, always clustered together with strong bootstrap support.

DISCUSSION

Cryptosporidium spp. and the origin of gregarines

Cryptosporidians were originally considered to be unusual coccidians (Fayer et al., 1997); however, recent molecular phylogenies based on SSU rRNA and several protein-coding genes suggest that cryptosporidians are early-diverging apicomplex-

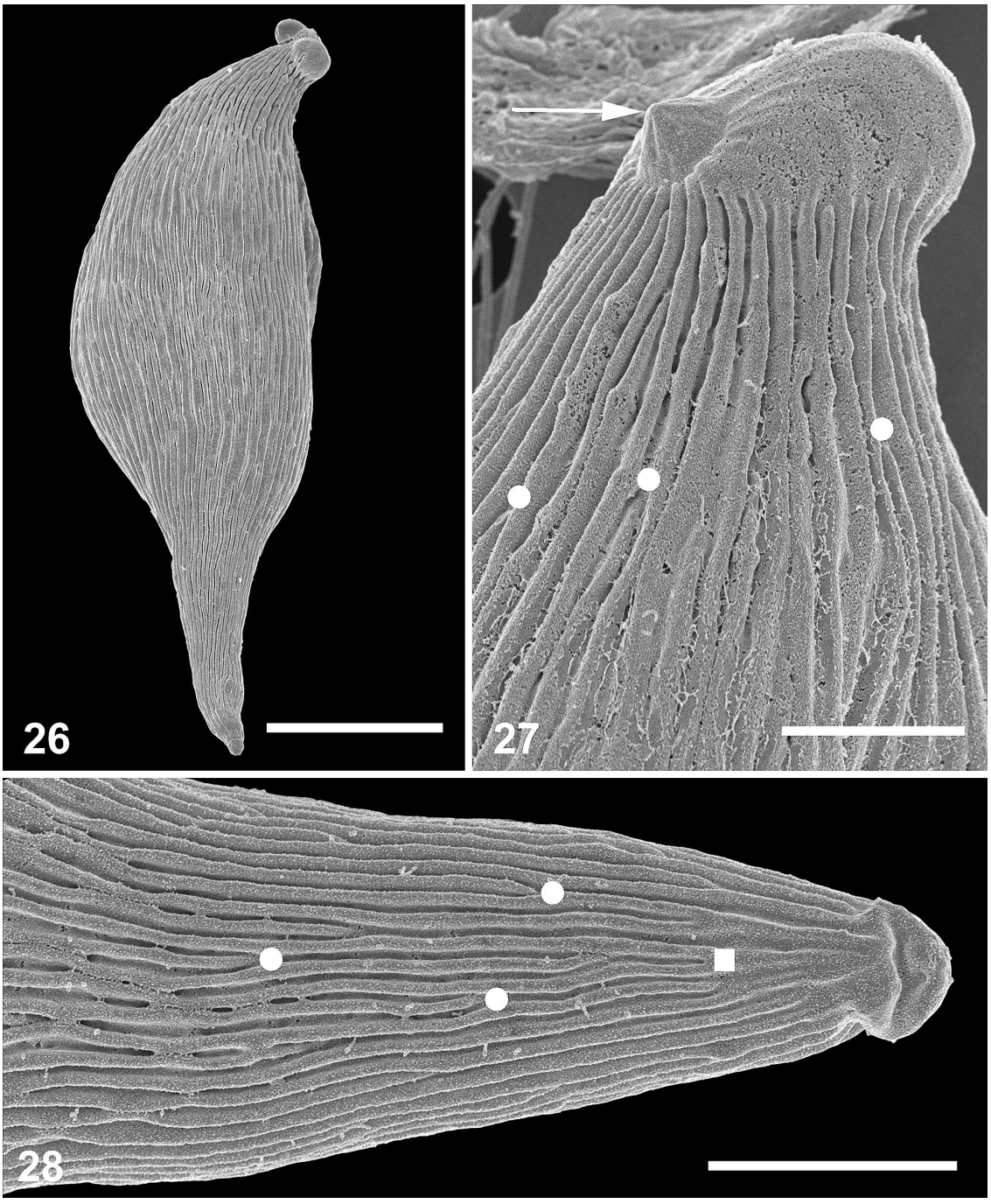

FIGURES 26–28. Scanning electron micrographs of *Monocystis agilis*. **26.** A lemon-shaped trophozoite showing longitudinally arranged cortex folds with a density of about 1–2 folds/μm. **27.** High-magnification view of the mucron showing folds that terminate before reaching the anterior end of the cell (circles) and a cone-shaped structure assumed to function in attachment (arrow). **28.** High-magnification view of the trophozoite showing folds that both terminate (circles) and bifurcate (squares) before the posterior cell apex. **26:** Bar = 20 μm. **27–28:** Bar = 5 μm.

ans with affinities to gregarines (Carreno et al., 1999; Zhu et al., 2000; Leander et al., 2003). Our phylogenetic analyses, in particular those including the more conserved sequence from the archigregarine *S. terebellae*, significantly bolster this hypothesis (Fig. 29B). However, despite the inclusion of 2 sequences from archigregarines (*S. terebellae* and *S. vivax*), cryptosporidians continue to diverge before all true gregarine sequences, making it impossible to distinguish between cryptosporidians as sisters to gregarines and cryptosporidians actually evolving from gregarines. The sequences from the marine parasite of *T. crocea* and the marine clone misattributed to *A. beccarii*, which were inferred to be gregarines in previous analyses (Pawlowski et al., 1996; Nakayama et al., 1998; Kuvardina et al., 2002; Leander et al., 2003), consistently diverged before the true gregarine clade (including *Cryptosporidium* spp.) in our analyses (Fig. 29). It is possible, therefore, that these 2 sequenc-

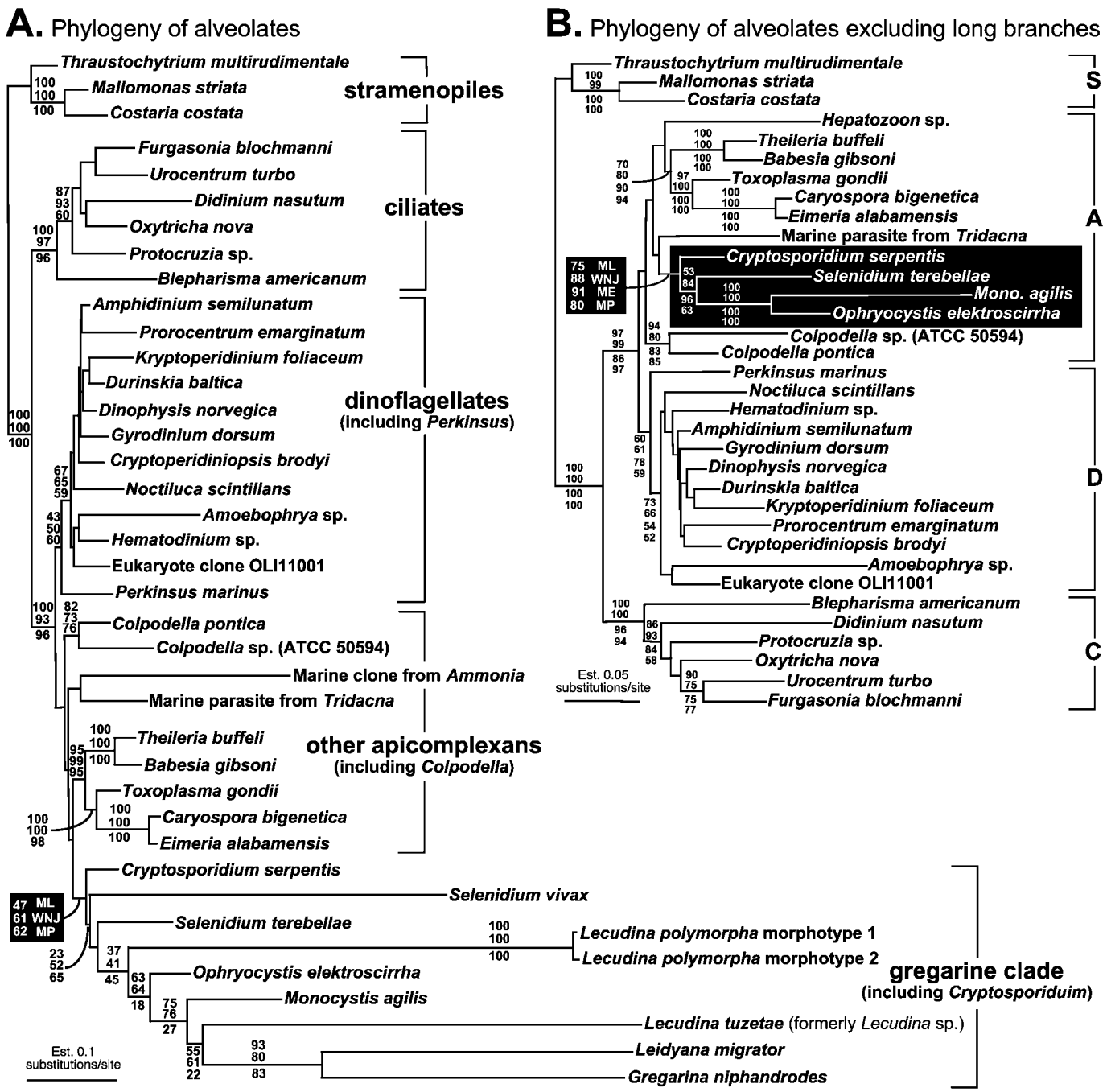

FIGURE 29. Phylogenetic trees showing the relationship of gregarines to other alveolates as inferred from SSU rDNA sequences. Numbers at the branches denote gamma-corrected bootstrap percentages of 100 replicates using the following methods (from top to bottom): ML, using HKY; weighted neighbor joining (WNJ); and minimum evolution (ME), using GTR; the lowermost numbers refer to 500 bootstrap replicates using maximum parsimomy (MP). **A.** Gamma-corrected ML tree ($-\ln L = 17{,}209.88$) inferred using the GTR model of substitution on an alignment of 40 SSU rDNA sequences and 1,408 sites—the 40-taxon alignment. Most gregarine sequences are extremely divergent and cluster with *Cryptosporidium serpentis* with moderate statistical support. **B.** Gamma-corrected ML tree ($-\ln L = 12{,}828.094$) inferred using the GTR model of substitution on an alignment of 34 SSU rDNA sequences and 1,435 sites—the 34-taxon alignment; the 6 longest branches have been removed from the 40-taxon alignment: *Selenidium vivax*, *Lecudina polymorpha* morphotype 1, *Lecudina polymorpha* morphotype 2, *Lecudina tuzetae*, *Leidyana migrator*, and *Gregarina niphandrodes*. In the absence of long branches, *C. serpentis* clusters with *Selenidium terebellae*, *Monocystis agils*, and *Ophryocystis elektroscirrha* with moderate to high statistical support (75/88/91/80). A, apicomplexans and *Colpodella*; C, ciliates; D, dinoflagellates and *Perkinsus*; S, stramenopiles.

es represent some of the earliest diverging gregarines and provide evidence that cryptosporidians are indeed derived from within the group, extending the range of gregarine hosts into vertebrates. However, it is also possible that these sequences come from an unrecognized form of apicomplexan parasite that would not be considered a gregarine. More information is needed about the biology of the *T. crocea* and *A. beccarii* parasites before any confident argument based on this tree topology alone can be developed (Fig. 29B).

Nevertheless, cryptosporidians are similar to gregarines in many notable respects, i.e., known species mostly infect epithelial cells of the host intestine and have nonmotile zygotes; moreover, *Cryptosporidium* spp. and many gregarines have life cycles with all 3 schizogonies (merogony, gametogony, and sporogony) (Fayer et al., 1997; Carreno et al., 1999). Like colpodellids and archigregarines (*Selenidium*), cryptosporidians have 4 infective zoites within each cyst, whereas all other gregarines have 8 or more sporozoites per cyst (Schrével, 1968, 1970, 1971a, 1971b; Brugerolle and Mignot, 1979; Simpson and Patterson, 1996; Fayer et al., 1997; Brugerolle, 2002; Perkins et al., 2002). This appears to be an important symplesiomorphy that fortifies the early phylogenetic position of *Cryptosporidium* spp. in molecular phylogenies. This early-diverging position is also consistent with the fact that cryptosporidians lack more derived features of gregarines, such as syzygy, epimerites, and large trophozoites with cortex folds and ectoplasmic septa.

Both cryptosporidians and some archigregarines inhabit deuterostomes from both marine and terrestrial environments (Levine, 1971; Fayer et al., 1997; Alvarez-Pellitero and Sitja-Bobadilla, 2002). This has led some authors to suggest that perhaps archigregarines, e.g., *Selenidium* spp., by affiliation, are more derived than previously assumed (Carreno et al., 1999). However, an interpretation that the deuterostome hosts of some archigregarines and cryptosporidians are qualitatively more derived than the protostome hosts of eugregarines and neogregarines, e.g., insects, is almost certainly based on anthropocentric assumptions. Many archigregarines, regardless of how they are defined (Levine, 1971; Schrével, 1971a, 1971b), also inhabit a variety of protostomes. There is every reason to suspect that archigregarines have retained a number of plesiomorphic features and perhaps form a paraphyletic group from which cryptosporidians, urosporidians (*Pterospora* spp.), and eugregarines (lecudinids, monocystids, and septate gregarines) have diverged independently. Moreover, it would not be surprising if the earliest diverging gregarines were eventually shown to be paraphyletic to all other apicomplexans. Molecular phylogenetic analyses including many *Selenidium* spp., particularly from deuterostome hosts, will shed considerable light on this issue.

Character-state transformations in the evolution of gregarine trophozoites

Selenidium spp., like all recognized archigregarines, have trophozoite stages that are very similar to sporozoite stages in both morphology and behavior. The trophozoites of *S. terebellae*, for instance, possess a relatively unfolded cortex and a conoidal anterior end with ringlike indentations reminiscent of the trichocyst openings of dinoflagellates (Figs. 9, 10). Ray (1930) described 'refringent threadlike bodies' within the cone-shaped anterior end of different *Selenidium* species by LM, but at the time, put forth no hypothesis about their function. Transmission electron microscopical studies of the trophozoites from different species of *Selenidium* (Schrével and Vivier, 1966; Schrével, 1968, 1971a, 1971b; Perkins et al., 2002) clearly indicate that the ringlike indentations, as seen by SEM (Fig. 10), and the threadlike bodies observed using LM (Ray, 1930; Schrével, 1970) are rhoptries. Thus, a common property of many *Selenidium* species is a trophozoite stage with a well-developed apical complex. Sporozoites use the apical complex for cell attachment and intracellular invasion, but the trophozoites of certain archigregarines, e.g., species of *Selenidium* and *Digyalum*, appear to use an apical complex to suck out the cytoplasm of host epithelial cells (Schrével and Vivier, 1966; Schrével, 1968; Dyson et al., 1994). This myzocytotic mode of feeding is strikingly similar to that found in colpodellids and some dinoflagellates, which feed on the cytoplasm of other unicellular eukaryotes, such as cryptomonads, chrysomonads, and bodonids (Myl'nikov, 1991, 2000; Simpson and Patterson, 1996; Brugerolle, 2002).

In eugregarines, the well-developed apical complex of sporozoites is lost during trophozoite development. This ontogenetic modification is correlated with the development of an elaborately folded cortex, suggesting that in eugregarines a mode of nutrition dependent on surface area replaced myzocytosis. The cortex folds of eugregarine trophozoites are likely structural adaptations that create the surface area necessary to effectively absorb nutrients passing through the host's intestinal tract (Cox, 1965). Our phylogenetic analyses suggest that an elaborately folded cortex evolved a single time because *Lecudina* spp., *Monocystis* spp., *Leidyana* spp., and *Gregarina* spp. form a monophyletic group in most analyses (Fig. 29). Little is known about the cortex morphology of the neogregarine *O. elektroscirrha*, but its SSU rDNA sequence suggests that it evolved from eugregarines with cortical folds. Species of *Lecudina*, as represented by *L. polymorpha*, appear to be 1 of the early lineages with trophozoites lacking an apical complex but possessing cortical folds. However, *Lecudina* contains more than 42 species encompassing almost every marine aseptate gregarine having rigid trophozoites with cortex folds and gliding motility (Levine, 1976). The genus, therefore, is probably paraphyletic, perhaps giving rise to many different recognized lineages of eugregarines independently. The sisterhood of *L. tuzetae* with septate gregarines in SSU rDNA phylogenies supports this point of view, although the relationship is tenuous.

The morphology of cortex folds can vary considerably, which may be important indicators of phylogenetic relationships. For instance, the trophozoite cortex of *Nematocystis* sp. is quite complex, consisting of a superfolded cortex in contracted stages of peristalticlike movements (Vávra and Small, 1969; MacMillan, 1973). Some species of *Selenidium*, e.g., *Selenidium fallax*, have an alternating pattern of deep and shallow grooves across the cortex (MacGregor and Thomas, 1965). *Rhynchocystis* sp. has an alternating pattern of elevated primary folds and shorter secondary folds (roughly 65 folds in total) that are on occasion anastomose with adjacent folds (Warner, 1968). In this case, the height of the folds varies rather than the depth of the grooves. Cortex folds also give rise to other cortical structures, such as undulating membranes, which do not appear to be involved in locomotion but rather in increasing

surface area for nutritional absorption (MacGregor and Thomas, 1965; Castellón and Gracia, 1988). Long cylindrical extensions, called cytopilia, emanate from the folds of many different gregarines, but their function is less clear (Lacy and Miles, 1959; Warner, 1968). Moreover, as the cortex folds of eugregarines extend into the posterior and anterior ends of the cell, some folds terminate or bifurcate before reaching the cell terminus (Figs. 19, 20, 25, 27, 28). This phenomenon is reminiscent of cell surface patterns formed by terminating strips on the pellicles of phototrophic euglenids (Leander et al., 2001). However, unlike euglenids, no distinct pattern of terminating and bifurcating folds was observed that could provide insights about phylogenetic relationships.

Gliding motility in the rigid trophozoites of eugregarines is inferred to result from at least 2 different mechanisms involving undulations of the cortex folds. First, in aseptate eugregarines, such as *L. tuzetae* and *L. pellucida* (Vivier, 1968), individual undulating folds are bordered on either side by a straight fold. The oblique surfaces of undulating folds move posteriorly and push on mucus within the space defined by the bordering straight folds, which drives the trophozoite forward. The straight folds also function as skates for gliding. Second, in septate gregarines, adjacent folds undulate 180° out of phase in a horizontal plane, causing the peaks of the folds to converge and thus produce a common surface that pushes posteriorly onto the surrounding mucilage (Vávra and Small, 1969).

The cortex folds of *M. agilis* lacked undulations (Figs. 26–28), which is consistent with their apparent inability to glide. By contrast, gliding did occur in both morphotypes of *L. polymorpha*, but their individual cortex folds were much straighter and more tightly packed than the folds reported from *L. tuzetae*, *L. pellucida*, and septate eugregarines (Vávra and Small, 1969) (Figs. 17–20, 23, 25). Presumably, localized regions of undulating folds provide a mechanism for gliding that is similar to that described for other species of *Lecudina* and for septate eugregarines. However, we were unable to document these regions in our sample. Alternatively, the presence of undulating folds may be reflective of earlier stages in trophozoite ontogeny. This is consistent with observations of *Gregarina* spp., where older trophozoites had straighter folds than their younger counterparts (Heller and Weise, 1973).

The SSU rDNA sequences from the 2 morphotypes of *L. polymorpha* were 99.3% identical. Furthermore, 1 of the 3 sequences from morphotype 2 was 100% identical to all the sequences from morphotype 1. This result can be interpreted in 2 ways. One possibility is that the DNA extracted from isolated trophozoites of morphotype 2 was contaminated with trophozoites of morphotype 1. However, this source of error is unlikely because extreme caution was taken when the cell isolations were conducted. A second possibility is that 2 populations of *L. polymorpha* exist within the host, each having a range of morphological variations encompassing both morphotypes. In this case, morphotypes 1 and 2 would represent 2 stages in trophozoite development from the sporozoite stage. Even though morphotype 2 is often longer and sometimes possessed an elongated mucron, variation in trophozoite width was identical in both morphotypes (range, 35–55 μm). The fold terminations and bifurcations on morphotype 2 of *L. polymorpha* appeared to be a biomechanical consequence of 'optimal packing' because the folds did not vary in thickness as the cell width narrowed near the posterior end (Fig. 25).

The cortex of archigregarine trophozoites is significantly different from those found in eugregarines, e.g., *Monocystis* spp., *Lecudina* spp., and *Gregarina* spp. For instance, the trophozoites of *S. vivax*, which are more similar to *Exoschizon siphonosomae* Hukui than to most members of *Selenidium*, have about 13 weak longitudinal striations on 1 side and peculiar writhing motility (Figs. 3, 13). The surface is also ornamented with transverse striations (Figs. 13–16) that are like and perhaps homologous to those described on *Digyalum oweni* Koura et al., an aseptate gregarine from littorinid gastropods (Dyson et al., 1993, 1994). Although the size of the transverse striations is consistent with epibiotic bacteria, they are more likely uniform wrinkles derived from the cortex itself because the ends of the striations were usually fused with the outer membrane (Fig. 14). Descriptions of the transverse striations using transmission electron microscopy are needed to clarify the issue. However, the other species of *Selenidium* we examined, *S. terebellae*, also possessed transverse striations that were clearly not of episymbiotic origin (Figs. 9, 11). The possession of transverse striations may be homologous in these species, but a larger sampling of *Selenidium* species is needed to more confidently evaluate this inference.

The presence and number of longitudinal striations, which are not 'optical illusions' as suggested by other authors (Levine, 1971), appear to vary considerably (4 to more than 90) in species classified in *Selenidium* (Ray, 1930; MacGregor and Thomas, 1965; Levine, 1971). Some species have very shallow longitudinal striations (folds) that come and go depending on the contractile behavior of the trophozoite, e.g., *S. vivax*; some have 4–16 wide, rounded folds in cross section (Ray, 1930; Vivier and Schrével, 1964), and some have about 40–50 folds that are more developed (Schrével, 1971a). Eugregarines, on the other hand, have well-defined folds that number into the hundreds (Vivier, 1968; Vávra and Small, 1969; Heller and Weise, 1973). It will be interesting from both evolutionary and taxonomic perspectives to know whether this diversity reflects phylogenetic relationships, particularly if *Selenidium* species with more folds are more closely related to eugregarines and if species of *Selenidium* with fewer folds are more closely related to cryptosporidians. It will also be important to understand the distinctions and potential homology between the cortex folds of eugregarines and the simpler striations of archigregarines. Answers to these questions will require a better understanding of the fundamental construction of the trophozoite cortex, how different cortex morphologies relate to different host compartments, e.g., intestinal lumen versus coelom, and the phylogeny of gregarines.

ACKNOWLEDGMENTS

We thank J. M. Archibald for comments on the manuscript. This work was supported by a grant to P.J.K. from the Canadian Institutes for Health Research (MOP-42517) and to B.S.L. from the National Science Foundation (Postdoctoral Research Fellowship in Microbial Biology). P.J.K. is a scholar of the Canadian Institute for Advanced Research, Canadian Institutes for Health Research, and the Michael Smith Foundation for Health Research.

LITERATURE CITED

ALVAREZ-PELLITERO, P., AND A. SITJA-BOBADILLA. 2002. *Cryptosporidium molnari* n. sp (Apicomplexa: Cryptosporidiidae) infecting two

marine fish species, *Sparus aurata* L. and *Dicentrarchus labrax* L. International Journal for Parasitology **32:** 1007–1021.

BRUGEROLLE, G. 2002. *Colpodella vorax*: Ultrastructure, predation, life-cycle, mitosis, and phylogenetic relationships. European Journal of Protistology **38:** 113–126.

———, AND J. P. MIGNOT. 1979. Observations sur le cycle l'ultrastructure et la position systématique de *Spiromonas perforans* (*Bodo perforans* Hoolande 1938), flagellé parasite de *Chilomonas paramecium*: Ses relations avec les dinoflagellés et sporozoaires. Protistologica **15:** 183–196.

BRUNO, W. J., N. D. SOCCI, AND A. L. HALPERN. 2000. Weighted neighbor joining: A likelihood-based approach to distance-based phylogeny reconstruction. Molecular Biology and Evolution **17:** 189–197.

CARRENO, R. A., D. S. MARTIN, AND J. R. BARTA. 1999. *Cryptosporidium* is more closely related to the gregarines than to coccidia as shown by phylogenetic analysis of apicomplexan parasites inferred using small-subunit ribosomal RNA gene sequences. Parasitology Research **85:** 899–904.

CASTELLÓN, C., AND M. D. GRACIA. 1988. *Lecudina capensis* sp. n., parasitic gregarine of *Pherusa laevis* Stimpson, 1856 (Polychaete Annelid). Acta Protozoologica **27:** 291–296.

COX, F. E. G. 1994. The evolutionary expansion of the sporozoa. International Journal for Parasitology **24:** 1301–1316.

COX, V. A. 1965. Movement in *Ditrypanocystis cirratuli*. Journal of Protozoology **12**(Suppl.): 3.

DESPORTES, I., AND J. THÉODORIDÈS. 1979. Étude ultrastructurale d'*Amphiamblys laubieri* n. sp. (Microsporidie, Metchnikovellidae) parasite d'une grégarine (*Lecudina* sp.) d'un echiurien abyssal. Protistologica **15:** 435–457.

DYSON, J., J. GRAHAME, AND P. J. EVENNETT. 1993. The mucron of the gregarine *Digyalum oweni* (Protozoa, Apicomplexa), parasitic in *Littorina* species (Mollusca, Gastropoda). Journal of Natural History **27:** 557–564.

———, ———, AND ———. 1994. The apical complex of the gregarine *Digyalum oweni* (Protozoa, Apicomplexa). Journal of Natural History **28:** 1–7.

FAYER, R., C. A. SPEER, AND J. P. DUBEY. 1997. The general biology of *Cryptosporidium*. *In* Cryptosporidium and cryptosporidiosis, R. Fayer (ed.). CRC Press, Boca Raton, Florida, p. 1–41.

FELSENSTEIN, J. 1993. PHYLIP: Phylogeny inference package. University of Washington, Seattle, Washington.

GRASSÉ, P.-P. 1953. Classe des grégarinomorphes (Gregarinomorpha n. nov.; Gregarinae Haeckel, 1866; gregarinidea Lankester, 1885; grégarines des auteurs). *In* Traité de Zoologie, P.-P. Grassé (ed.). Masson, Paris, France, p. 590–690.

GUNDERSON, J., AND E. B. SMALL. 1986. *Selenidium vivax* n. sp. (Protozoa, Apicomplexa) from the sipunculid *Phascolosoma agassizii* Keferstein, 1867. Journal of Parasitology **72:** 107–110.

HELLER, G., AND R. W. WEISE. 1973. A scanning electron microscope study on *Gregarina* sp. from *Udeopsylla nigra*. Journal of Protozoology **20:** 61–64.

KUVARDINA, O. N., B. S. LEANDER, V. V. ALESHIN, A. P. MYL'NIKOV, P. J. KEELING, AND T. G. SIMDYANOV. 2002. The phylogeny of colpodellids (Eukaryota, Alveolata) using small subunit rRNA genes suggests they are the free-living ancestors of apicomplexans. Journal of Eukaryotic Microbiology **49:** 498–504.

KUZNETSOV, S. A., G. M. LANGFORD, AND D. G. WEISS. 1992. Actin-dependent organelle movement in squid axoplasm. Nature **356:** 722–725.

LACY, D., AND H. B. MILES. 1959. Observations by electron microscopy on the structure of an acephaline gregarine (*Apolocystis elnogata* Phillips and Mackinnon). Nature **183:** 1456–1457.

LEANDER, B. S., R. E. CLOPTON, AND P. J. KEELING. 2003. Phylogeny of gregarines (Apicomplexa) as inferred from SSU rDNA and beta-tubulin. International Journal of Systematic and Evolutionary Microbiology **53:** 345–354.

———, AND P. J. KEELING. 2003. Morphostasis in alveolate evolution. Trends in Ecology and Evolution **18:** 395–402.

———, R. P. WITEK, AND M. A. FARMER. 2001. Trends in the evoluton of the euglenid pellicle. Evolution **55:** 2115–2135.

LEVINE, N. D. 1971. Taxonomy of the Archigregarinorida and Selenidiidae (Protozoa, Apicomplexa). Journal of Protozoology **18:** 704–717.

———. 1974. Gregarines of the genus *Lecudina* (Protozoa, Apicomplexa) from pacific ocean polychaetes. Journal of Protozoology **21:** 10–12.

———. 1976. Revision and checklist of the species of the aseptate gregarine genus Lecudina. Transactions of the American Microscopical Society **95:** 695–702.

MACGREGOR, H. C., AND P. A. THOMAS. 1965. The fine structure of two archigregarines, *Selenidium fallax* and *Ditrypanocystis cirratuli*. Journal of Protozoology **12:** 438–443.

MACMILLAN, W. G. 1973. Conformational changes in the cortical region during peristaltic movements of a gregarine trophozoite. Journal of Protozoology **20:** 267–274.

MADDISON, D. R., AND W. P. MADDISON. 2000. MacClade. Sinauer Associates, Inc., Sunderland, Massachusetts.

MYL'NIKOV, A. P. 1991. The ultrastructure and biology of some representatives of order Spiromonadida (Protozoa). Zoologichesky Zhurnal **70:** 5–15.

———. 2000. The new marine carnivorous flagellate *Colpodella pontica* (Colpodellida, Protozoa). Zoologichesky Zhurnal **79:** 261–266.

NAKAYAMA, K., M. NISHIJIMA, AND T. MARUYAMA. 1998. Parasitism by a protozoan in the hemolymph of the giant clam, *Tridacna crocea*. Journal of Invertebrate Pathology **71:** 193–198.

PAWLOWSKI, J., I. BOLIVAR, J. F. FAHRNI, T. CAVALIER-SMITH, AND M. GOUY. 1996. Early origin of Foraminifera suggested by SSU rRNA gene sequences. Molecular Biology and Evolution **13:** 445–450.

PERKINS, F. O., J. R. BARTA, R. E. CLOPTON, M. A. PEIRCE, AND S. J. UPTON. 2002. Phylum Apicomplexa. *In* The illustrated guide to the protozoa, J. J. Lee, G. F. Leedale, and P. Bradbury (eds.). Allen Press, Inc., Lawrence, Kansas, p. 190–304.

POSADA, D., AND K. A. CRANDALL. 1998. MODELTEST: Testing the model of DNA substitution. Bioinformatics **14:** 817–818.

RAY, H. N. 1930. Studies on some protozoa in polychaete worms. I. Gregarines of the genus *Selenidium*. Parasitology **22:** 370–400.

SCHNEPF, E., AND G. DEICHGRABER. 1984. ''Myzocytosis'', a kind of endocytosis with implications to compartmentalization in endosymbiosis: Observations on *Paulsenella* (Dinophyta). Naturwissenschaften **71:** 218–219.

SCHRÉVEL, J. 1963. Grégarines nouvelles de Nereidae et Eunicidae (Annélides, Polychètes). Comptes Rendus de la Societe de Biologie **157:** 814–816.

———. 1968. L'ultrastructure de la région antérieure de la grégarine *Selenidium* et son intérêt pour l'étude de la nutrition chez les sporozoaires. Journal de Microscopie **7:** 391–410.

———. 1969. Recherches sur le cycle des Lecudinidae grégarines parasites d'annélides polychétes. Protistologica **5:** 561–588.

———. 1970. Contribution a l'étude des Selenidiidae parasites d'annélides polychètes. I. Cycles biologiques. Protistologica **6:** 389–426.

———. 1971a. Contribution a l'étude des Selenidiidae parasites d'annélides polychètes. II. Ultrastructure de quelques trophozoïtes. Protistologica **7:** 101–130.

———. 1971b. Observations biologique et ultrastructurales sur les Selenidiidae et leurs conséquences sur la systématique des grégarinomorphes. Journal of Protozoology **18:** 448–470.

———, AND E. VIVIER. 1966. Étude de l'ultrastructure et du rôle de la région antérieure (mucron et épimerite) de grégarines parasites d'annélides polychètes. Protistologica **2:** 17–28.

SIMPSON, A. G. B., AND D. J. PATTERSON. 1996. Ultrastructure and identification of the predatory flagellate *Colpodella pugnax* Cienkowski (Apicomplexa) with a description of *Colpodella turpis* n. sp. and a review of the genus. Systematic Parasitology **33:** 187–198.

STRIMMER, K., AND A. VON HAESELER. 1996. Quartet puzzling: A quartet maximum likelihood method for reconstructing tree topologies. Molecular Biology and Evolution **13:** 964–969.

SWOFFORD, D. L. 1999. PAUP*: Phylogenetic analysis using parsimony (and other methods), version 4.0. Sinauer Associates, Inc., Sunderland, Massachusetts.

THÉODORIDÈS, J. 1984. The phylogeny of the Gregarinia. Origins of Life **13:** 339–342.

VÁVRA, J., AND E. B. SMALL. 1969. Scanning electron microscopy of gregarines (Protozoa, Sporozoa) and its contribution to the theory of gregarine movement. Journal of Protozoology **16:** 745–757.

VIVIER, E. 1968. L'organization ultrastructurale corticale de la gregarine

Lecudina pellucida: Ses repports avec l'alimentation et la locomotion. Journal of Protozoology **15:** 230–246.

———. 1975. The microsporidia of the protozoa. Protistologica **11:** 345–361.

———, AND I. DESPORTES. 1990. Phylum Apicomplexa. *In* The handbook of Protoctista, L. Margulis, J. O. Corliss, M. Melkonian, and D. J. Chapman (eds.). Jones and Bartlett Publishers, Boston, Massachusetts, p. 549–573.

———, AND J. SCHRÉVEL. 1964. Étude, au microscope électronique, d'une grégarine du genre *Selenidium*, parasite de *Sabellaria alveolata* L. Journal de Microscopie **3:** 651–670.

WARNER, F. D. 1968. The fine structure of *Rhynchocystis pilosa* (Sporozoa, Eugregarinida). Journal of Protozoology **15:** 59–73.

ZHU, G., J. S. KEITHLY, AND H. PHILIPPE. 2000. What is the phylogenetic position of *Cryptosporidium*? International Journal of Systematic and Evolutionary Microbiology **50:** 1673–1681.

ZOLAN, M. E., AND P. J. PUKKILA. 1986. Inheritance of DNA methylation in *Coprinus cinereus*. Molecular and Cellular Biology **6:** 195–200.